2011

Structural and Functional Analysis of the Type III Secretion System from *Pseudomonas fluorescens* Q8r1-96

Dmitri V. Mavrodi
Washington State University, mavrodi@mail.wsu.edu

Anna Joe
University of Nebraska-Lincoln

Olga V. Mavrodi
Washington State University

Karl A. Hassan
Macquarie University, Sydney, Australia, karl.hassan@mq.edu.au

David M. Weller
USDA-ARS, Pullman, WA, david.weller@ars.usda.gov

See next page for additional authors

JOURNAL OF BACTERIOLOGY, Jan. 2011, p. 177–189 Vol. 193, No. 1
0021-9193/11/$12.00 doi:10.1128/JB.00895-10

Structural and Functional Analysis of the Type III Secretion System from *Pseudomonas fluorescens* Q8r1-96▽§

Dmitri V. Mavrodi,[1]† Anna Joe,[2]† Olga V. Mavrodi,[1] Karl A. Hassan,[4] David M. Weller,[3] Ian T. Paulsen,[4] Joyce E. Loper,[5] James R. Alfano,[2] and Linda S. Thomashow[3]*

Department of Plant Pathology, Washington State University, Pullman, Washington 99164-6430[1]; Center for Plant Science Innovation and Department of Plant Pathology, University of Nebraska, Lincoln, Nebraska 68588-0660[2]; USDA Agricultural Research Service, Root Disease and Biological Control Research Unit, Pullman, Washington 99164-6430[3]; Department of Chemistry and Biomolecular Sciences, Macquarie University, Sydney, Australia[4]; and USDA Agricultural Research Service, Horticultural Crops Research Laboratory, Corvallis, Oregon 97330[5]

Received 29 July 2010/Accepted 11 October 2010

***Pseudomonas fluorescens* Q8r1-96 represents a group of rhizosphere strains responsible for the suppressiveness of agricultural soils to take-all disease of wheat. It produces the antibiotic 2,4-diacetylphloroglucinol and aggressively colonizes the roots of cereal crops. In this study, we analyzed the genome of Q8r1-96 and identified a type III protein secretion system (T3SS) gene cluster that has overall organization similar to that of the T3SS gene cluster of the plant pathogen *Pseudomonas syringae*. We also screened a collection of 30 closely related *P. fluorescens* strains and detected the T3SS genes in all but one of them. The Q8r1-96 genome contained *ropAA* and *ropM* type III effector genes, which are orthologs of the *P. syringae* effector genes *hopAA1-1* and *hopM1*, as well as a novel type III effector gene designated *ropB*. These type III effector genes encoded proteins that were secreted in culture and injected into plant cells by both *P. syringae* and Q8r1-96 T3SSs. The Q8r1-96 T3SS was expressed in the rhizosphere, but mutants lacking a functional T3SS were not altered in their rhizosphere competence. The Q8r1-96 type III effectors RopAA, RopB, and RopM were capable of suppressing the hypersensitive response and production of reactive oxygen species, two plant immune responses.**

Rhizosphere-inhabiting fluorescent *Pseudomonas* spp. have been studied extensively in recent years because they can provide biological control of soilborne pathogens of a wide range of agricultural crops and they have a key role in the suppressiveness of some soils to plant pathogens (66). Among the major phenotypic traits associated with biological control are the capacity to produce biologically active metabolites and the ability to colonize and persist in the plant rhizosphere. The latter trait is of critical importance because a successful biocontrol agent must establish and maintain a minimum threshold population density in order to provide effective protection of the host plant. Most rhizosphere isolates of *Pseudomonas* spp. readily colonize diverse plant species and establish populations large enough to suppress a variety of pathogens (66), but their populations decline over time to levels below the threshold needed for disease control. Others are characterized by extraordinarily competitive colonization of the roots of particular crops on which they maintain population sizes sufficient to provide extended disease suppression (66). Such superior root colonizers are exemplified by a group of strains of the *Pseudomonas fluorescens* complex that produce the polyketide antibiotic 2,4-diacetylphloroglucinol (2,4-DAPG) and belong to the rep-PCR D genotype (67). In order to gain insight into this superior root colonizer phenotype, we recently sequenced the genome of the D-genotype strain *P. fluorescens* Q8r1-96 and identified genes that encode, among traits potentially important in interactions with the host plant, a type III protein secretion apparatus.

Type III protein secretion systems (T3SSs) are found in many Gram-negative bacteria that live in close association with eukaryotes (18, 52). T3SSs act as molecular syringes that can inject bacterial proteins called type III effectors into eukaryotic cells (11, 14, 62, 71). Exactly how type III effectors are injected and what they target once inside host cells make up one of the most actively investigated areas of research in host-microbe interactions. The T3SSs of plant pathogens are encoded by the *hrp*/*hrc* gene cluster (2, 62). While the majority of plant targets for type III effectors remain unknown, it is becoming apparent that they are directed to components of the plant immune system (11, 25, 71).

Plant immunity can be broadly viewed as consisting of two main branches. One branch is triggered by conserved microbial compounds that are recognized outside the plant cell by extracellular receptors (12, 46). These molecules are found in both pathogenic and nonpathogenic microbes and are called pathogen (microbe)-associated molecular patterns (PAMPs/MAMPs) (7, 44). When a PAMP is recognized, it induces immune responses collectively referred to as PAMP-triggered immunity (PTI) (33). The other branch is induced by effector proteins from pathogens. These effectors are recognized by resistance (R) proteins, resulting in effector-triggered immunity (ETI). The majority of the research on plant immunity has been done on aerial plant parts. However, roots have recently been shown to induce PTI in response to specific PAMPs (45).

* Corresponding author. Mailing address: USDA Root Disease and Biocontrol Research Unit, Washington State University, Pullman, WA 99164-6430. Phone: (509) 335-3269. Fax: (509) 335-7674. E-mail: thomashow@wsu.edu.

§ Supplemental material for this article may be found at http://jb.asm.org/.

† These authors contributed equally to this study.

▽ Published ahead of print on 22 October 2010.

First investigated in the context of pathogenesis, T3SSs have recently been recognized as an essential feature of a wide range of mutualistic and commensal symbioses that arise from the colonization of eukaryotic hosts by Gram-negative bacteria (52). Pseudomonads represent an environmentally significant group of bacteria that often colonize higher organisms, and T3SSs are found in both pathogenic and saprophytic species of this genus. However, our understanding of the importance of the T3SS and its effectors for interactions of *Pseudomonas* spp. with eukaryotic hosts is largely limited to the opportunistic human and animal pathogen *Pseudomonas aeruginosa* (64) and the plant pathogen *Pseudomonas syringae* (3). The function of the T3SS in saprophytic members of this genus, and particularly in ubiquitous rhizosphere-dwelling *Pseudomonas* spp., remains poorly understood.

To date, the role of the T3SS in rhizosphere pseudomonads has been studied only in two isolates of the *P. fluorescens* complex. Rainey (55) and Preston et al. (53) identified and characterized a 20-kb gene cluster resembling the *hrp*/*hrc* locus of *P. syringae* in the sugar beet isolate *P. fluorescens* SBW25. While SBW25 has no known pathogenic activity, Preston et al. (53) showed that constitutive expression of its *hrpL* homolog enabled an AvrB-dependent hypersensitive response (HR) in *Arabidopsis* and a host-specific HR in *Nicotiana clevelandii*, suggesting that this T3SS is functional. Inactivation of T3SS genes compromised the ability of SBW25 to persist in the plant rhizosphere. A T3SS was also characterized by Rezzonico et al. (56) in *P. fluorescens* KD, which controls the oomycete *Pythium ultimum* and has no known phytopathogenic activity. Inactivation of this strain's T3SS strongly reduced its activity against *Pythium ultimum* on cucumber but had no measurable effect on root colonization (56). No type III effectors were identified in *P. fluorescens* KD, and the exact function of type III effectors in SBW25 has remained elusive. The lack of information from other rhizosphere isolates has provided few clues about the diversity of T3SSs and type III effectors that are associated with the rhizosphere lifestyle.

Here, we bridge this gap in our knowledge by reporting the sequence and organization of the T3SS cluster from *P. fluorescens* Q8r1-96, which produces 2,4-DAPG and is representative of strains responsible for the suppressiveness of U.S. and European agricultural soils to take-all disease of wheat (66, 67). We describe novel type III effectors from *P. fluorescens* and present evidence that these effectors, like their *P. syringae* counterparts, are capable of suppressing PAMP- and effector-triggered plant immunity. Finally, we show that Q8r1-96-like T3SS genes are widely distributed and highly conserved among rhizosphere isolates of *Pseudomonas* spp. of diverse geographic and host plant origin.

MATERIALS AND METHODS

Bacterial strains and plasmids. Strains and plasmids used in this study are listed in Table 1. Strains of 2,4-DAPG-producing *Pseudomonas* spp. screened for the presence of T3SS were described previously (40) and include CHA0, Pf-5, Q2-1, Q2-2, Q2-5, Q2-87, Q37-87, QT1-5, QT1-6, W2-6, W4-4, D27B1, JMP6, JMP7, FFL1R18, CV1-1, HT5-1, FTAD1R36, FL1R22, 7MA12, MVW1-1, MVW4-2, MVP1-4, STAD384, FTAD1R34, FFL1R9, Q128-87, OC4-1, ATCC 49054, and F113. *Pseudomonas* spp. and *Escherichia coli* were grown at 28°C and 37°C, respectively, in Luria-Bertani (LB) (8), M9 (8), or one-third-strength King's medium B (KMB) (34). For type III secretion assays, *Pseudomonas* spp. were grown in Hrp-inducing minimal medium at 22°C (30). Antibiotic supplements were used at the following concentrations: chloramphenicol (Cm), 30 μg/ml; gentamicin (Gm), 10 or 12 μg/ml; rifampin (Rif), 100 μg/ml; spectinomycin (Sp), 50 μg/ml; tetracycline (Tc), 20 μg/ml; and kanamycin (Km), 25 μg/ml.

Sequence analyses. DNA sequence data were analyzed with Vector NTI Advance 9 (Invitrogen, Carlsbad, CA) and OMIGA 2.0 (Accelrys, San Diego, CA). Database searches for similar protein sequences were performed using the NCBI's BLAST network service (http://www.ncbi.nlm.nih.gov/BLAST). Database searches against collections of protein motifs and domains were carried out by using the MyHits (49) and CD-Search (39) web-based engines. Protein folds and subcellular localization were predicted by using Phyre (10) and PSORTb 2.0 (23), respectively. The Q8r1-96 genome assembly (I. T. Paulsen et al., unpublished data) was screened for potential Hrp boxes using hidden Markov models (HMMs) built from the compilation of *P. syringae* Hrp box sequences using HMMER3 (http://hmmer.wustl.edu). Sequences of the Q8r1-96 *rsp*/*rsc* gene cluster and effector genes were deposited in GenBank under accession numbers HM991502 through HM991505.

Amplification of T3SS genes and phylogenetic inference. To screen 2,4-DAPG-producing *Pseudomonas* spp. for the presence of T3SS, genomic DNA was extracted from bacteria by using a cetyltrimethyl ammonium bromide miniprep procedure (8) and screened by PCR with HRCR8092–HRCT8986 and q8up–q8low primer sets (Table 1). Amplification was performed with a PTC-200 gradient thermal cycler (Bio-Rad, Hercules, CA) using GoTaq DNA polymerase (Promega, Inc., Madison, WI). The DNA fragments amplified by primers q8up and q8low were cleaned with QIAquick PCR purification spin columns (Qiagen, Valencia, CA) and sequenced with a BigDye Terminator v. 3.1 cycle sequencing kit (Applied Biosystems, Foster City, CA). The nucleotide sequences were aligned with Clustal X 2.0.9 (36), and Molecular Evolutionary Genetics Analysis (MEGA) software 4.0.2 (63) was used to infer neighbor-joining (NJ) trees. Reproducibility of clades within the inferred NJ trees was assessed by bootstrap resampling with 1,000 replicates.

Construction of expression plasmids. Standard techniques were used for plasmid DNA isolation, cloning, agarose gel electrophoresis, and electroporation (8). PCR amplifications were performed with KOD Hot Start DNA polymerase (Novagen, Madison, WI) according to the manufacturer's recommendations. Oligonucleotides were designed with Oligo 6.65 software (Molecular Biology Insights, West Cascade, CO).

For construction of pLN615-based plasmids, target genes were amplified with the primers listed in Table 1 and cloned into a pENTR/D-TOPO Gateway entry vector (Invitrogen) by following the manufacturer's recommendations. To clone genes *srcB* and *ropB* in tandem, the genes were amplified separately by PCR with primer sets srcB-up–srcB-low and ropB-up1–ropB-low (Table 1), and the two partially overlapping fragments were gel purified and fused by overlap extension PCR (16) with primers srcB-up and ropB-low. All pENTR/D-TOPO-based recombinant plasmids were single-pass sequenced to confirm the integrity of the cloned genes, and LR Clonase II enzyme (Invitrogen) was used to transfer the cloned genes into pLN615 (Table 1). The pLN615-based plasmids were introduced into *P. fluorescens* 55 by triparental mating.

Construction of *rsc*/*rsp* mutants and transposon tagging. Mutations in *rspL*, *rscV*, *rscC*, *ropB*, and *rspH* were introduced as follows. For each gene, sequences flanking the chosen cassette insertion site were amplified by PCR with corresponding m1-m2 and m3-m4 primer sets, and the Km^r cassette was amplified with primers Fkan and Rkan (Table 1). The partially overlapping fragments were gel purified with a QIAEX II gel extraction kit (Qiagen) and fused by overlap extension PCR (16) with KOD Hot Start DNA polymerase (Novagen) and primers m1 and m4. The resultant PCR fragments were cloned into the SmaI site of the gene replacement vector pEX18Tc.

To create the ΔOPQR and rscR mutants, pCR-T3SG2 (Table 1) was treated with HindIII, BamHI, and Klenow DNA polymerase I fragment and religated, yielding pCR-T3SG2Δ. For the ΔOPQR mutation, the pCR-T3SG2Δ plasmid was treated with PstI and T4 DNA polymerase and ligated with the 879-bp Gm^r cassette, giving pCR-T3SG2ΔPst. To inactivate *rscR*, pCR-T3SG2Δ was treated with SacI and T4 DNA polymerase and then ligated with the Gm^r cassette, yielding pCR-T3SG2ΔSac. The interrupted inserts from pCR-T3SG2ΔPst and pCR-T3SG2ΔSac were subcloned into pEX18Tc. All pEX18Tc-based plasmids were mobilized in Q8r1-96 from *E. coli* S17-1(λ-pir), and double crossover events were selected and verified by PCR as described earlier (42).

The *rspJ-luxCDABE* transcriptional fusion was constructed by amplifying the *rscJ* promoter with primers PrspJ3 and PrspJ4 (Table 1), digesting the resultant fragment with BamHI and PstI, and cloning it into pUC18-miniTn*7*T-Gm-*lux* (17). Q8r1-96 was tagged by electroporation of freshly prepared competent cells with 200 ng each of pUC18-miniTn*7*T-Gm-*lux-rspJ* and the helper plasmid pTNS2 (17). The tagged clones were isolated on LB agar amended with genta-

TABLE 1. Bacterial strains, plasmids, and oligonucleotide primers used in this study

Strain, plasmid, or oligonucleotide primer	Description[a]	Reference or source
P. fluorescens		
Q8r1-96	Wheat rhizosphere isolate from Quincy, WA; Rif^r	54
Q8r1-96Gm	Q8r1-96 tagged with mini-Tn*7*-*gfp2*; Rif^r Gm^r	65
Q8r1-96Km	Q8r1-96 tagged with mini-Tn*7*-*gfp1*; Rif^r Km^r	65
Q8r1-96rspL	T3SS mutant; *rspL*::*aph*; Rif^r Km^r	This study
Q8r1-96rscV	T3SS mutant; *rscV*::*aph*; Rif^r Km^r	This study
Q8r1-96rscR	T3SS mutant; *rscR*::*aacC1*; Rif^r Gm^r	This study
Q8r1-96ΔOPQR	T3SS mutant; Δ(*rspOP-rscQR)*::*aacC1*; Rif^r Gm^r	This study
Q8r1-96rscC	T3SS mutant; *rscC*::*aph*; Rif^r Km^r	This study
Q8r1-96ropB	T3SS mutant; *ropB*::*aph*; Rif^r Km^r	This study
Q8r1-96rspH	T3SS mutant; *rspH*::*aph*; Rif^r Km^r	This study
Q8r1-96rspJ-lux	Q8r1-96 tagged with mini-Tn*7*T-Gm-P_{rspJ}::*lux*; Rif^r Gm^r	This study
55	Nal^r	M. Sasser
Pseudomonas syringae		
DC3000	Wild type; spontaneous Rif^r	19
DC3000 *hrcC*	*hrcC* mutant defective in T3SS; Rif^r Cm^r	70
Escherichia coli		
S17-1(λ-pir)	*thi pro hsdM recA rpsL* RP4-2 (Tc^r::Mu) (Km^r::Tn*7*)	Laboratory collection
DH5α	F^- ϕ80*lacZ*ΔM15 Δ(*lacZYA-argF)U169 recA1 endA1 hsdR17* (r_K^- m_K^+) *gal phoA supE44* λ^- *thi-1 gyrA96 relA1*	Invitrogen
DB3.1	F^- *gyrA462 endA1* Δ(*sr1-recA*) *mcrB mrr hsdS20* (r_B^- m_B^-) *supE44 ara-14 galK2 lacY1 proA2 rpsL20* (Sm^r) *xyl-5* λ^- *leu mtl-1*	Invitrogen
Plasmids		
pUC18-mini-Tn*7*T-Gm-*lux*	Mini-Tn*7*-based transcriptional fusion vector with *luxCDABE* genes; Gm^r Amp^r	17
pTNS2	Tn*7* transposase donor; Amp^r	17
pUC18-mini-Tn*7*T-*lux-rspJ*	pUC18-mini-Tn*7*T-Gm-*lux* derivative with P_{rspJ}::*lux* transcriptional fusion; Gm^r Amp^r	This study
pHIR11	Cosmid pLAFR3 derivative carrying genomic DNA of *P.* syringae pv. syringae 61; Tc^r	29
pLN347	pML123 derivative containing *avrPtoB-ha*; Gm^r	32
pLN1965	pHIR11 derivative containing a deletion of *srcA*/*hopA1* operon that is replaced with Sp-resistant gene cassette; Tc^r Sp^r	25
pLN2193	pML123-derived Gateway destination vector containing a CyaA tag for C-terminal fusions; Gm^r	M. Guo
pCPP2318	Plasmid carrying *blaM* lacking signal peptide sequence; Tc^r	15
pLN4451	pML123 derivative containing $hopU1_{\Delta N15}$-*cyaA*; Gm^r	This study
pLN4452	pML123 derivative containing *ropAA-cyaA*; Gm^r	This study
pLN4453	pML123 derivative containing *srcM* and *ropM-cyaA*; Gm^r	This study
pLN4454	pML123 derivative containing *ropB-cyaA*; Gm^r	This study
pLN4455	pML123 derivative containing *srcB* and *ropB-cyaA*; Gm^r	This study
pENTR/D-TOPO	Entry vector for Gateway system; ColE1 Kan^r	Invitrogen
pLN615	pML123-derived destination vector for Gateway system for C-end HA tagging; Gm^r Cm^r	25
pLN615-M	pLN615 containing *srcM* and *ropM* from Q8r1-96; Gm^r	This study
pLN615-AA	pLN615 containing *ropAA* from Q8r1-96; Gm^r	This study
pLN615-B	pLN615 containing *ropB* from Q8r1-96; Gm^r	This study
pLN615-srcB	pLN615 containing a tandem of *srcB* and *ropB* genes from Q8r1-96; Gm^r	This study
pUCGM	Source of Gm^r cassette; ColE1 *bla aacC1*	26
pUC4K	Source of Km^r cassette; ColE1 *bla aph*	GE Healthcare
pEX18Tc	Gene replacement vector; Tc^r; $oriT^+$ $sacB^+$	26
pCR-Blunt	Cloning vector; Km^r Zeo^r ColE1 $ccdB^+$	Invitrogen
5D8	pCPP47-based cosmid with T3SS genes of Q8r1-96	This study
16E12	pCPP47-based cosmid with T3SS genes of Q8r1-96	This study
pCR-T3SG2	pCR-Blunt containing the 6,066-bp fragment with *rspQ* through *rscT* genes amplified by PCR with T3SG2 and q8up primers	This study
pCR-T3SG2Δ	pCR-T3SG2 containing the HindIII-BamHI deletion	This study
pCR-T3SG2ΔPst	pCR-T3SG2Δ with *rspOP-rscQR* replaced by the Gm^r cassette	This study
pCR-T3SG2ΔSac	pCR-T3SG2Δ with *rscR* interrupted by the Gm^r cassette	This study
pEX18Tc-ΔPst	pEX18Tc containing insert from pCR-T3SG2ΔPst	This study
pEX18Tc-ΔSac	pEX18Tc containing insert from pCR-T3SG2ΔSac	This study
Oligonucleotide primers		
PrspJ3	5′-CAT TGG ATC CTA GTG CTT TTG CTC TAT TTG TG-3′; upper primer for amplification of the *rspJ* promoter region; T_m, 78.2°C	This study
PrspJ4	5′-CTT GCT GCA GGA TCA GGT CGG TA-3′; lower primer for amplification of the *rspJ* promoter region; T_m, 73.5°C	This study
P_{Tn7R}	5′-CAC AGC ATA ACT GGA CTG ATT TC-3′; primer for amplification of the region flanking *att*Tn*7*; T_m, 64.1°C	17
Q8glmS	5′-AAC CTG GCG AAA TCT GTG AC-3′; primer for amplification of the region flanking *att*Tn*7*; T_m, 64.5°C	This study

Continued on following page

TABLE 1—*Continued*

Strain, plasmid, or oligonucleotide primer	Description[a]	Reference or source
q8up	5′-CGT CAT CTC CTT GAA CAG CAG-3′; upper primer for amplification of *rscRST* genes; T_m, 65.3°C	This study
q8low	5′-CTC GAC AGC CTC TTC TAT TCC-3′; lower primer for amplification of *rscRST* genes; T_m, 63.2°C	This study
HRCR8092	5′-CCI TTY ATC GTY ATY GAY YT-3′; upper primer for amplification of *rscRST* genes; T_m, 54.6-64.9°C	43
HRCT8986	5′-CTG TCC CAG ATI AIC TGI GT-3′; lower primer for amplification of *rscRST* genes; T_m, 56.1°C	43
T3SG2	5′-CAG ACC CAG ACG GAA AC-3′; upper primer for amplification of the 6,066-bp fragment spanning *rspQ* through *rscT* genes; T_m, 57.1°C	This study
ropAA-up	5′-CAC CAC AAG AGA CCC GCC CAT GGA TTC-3′; upper primer for amplification of the 1,327-bp fragment with *ropAA*; T_m, 83.2°C	This study
ropAA-low	5′-AAC AGC TCG CTC GGC GGC ATT G-3′; lower primer for amplification of the 1,327-bp fragment with *ropAA*; T_m, 80.4°C	This study
srcM-up	5′-CAC CAA TGC GAG GTC ACT CAT GGC GTC-3′; upper primer for amplification of the 2,634-bp fragment with *srcM* and *ropM*; T_m, 83.4°C	This study
ropM-low	5′-GCT TGG CCG GGT AGT GGG TGC AG-3′; lower primer for amplification of the 2,634-bp fragment with *srcM* and *ropM*; T_m, 80.7°C	This study
srcB-up	5′-CAC CAG GGA GGT TTC CCA TGA CCG TC-3′; upper primer for amplification of the 485-bp fragment with *srcB*; T_m, 81.6°C	This study
srcB-low	5′-ACG AGT CGA TGT CTG TGT CTA TCC CAA TCG GGT GCG GC-3′; lower primer for amplification of the 485-bp fragment with *srcB*; T_m, 93.9°C	This study
ropB-up	5′-CAC CGA CTC GTG GAG GAT TCC CAT GCC-3′; upper primer for amplification of the 523-bp fragment with *ropB*; T_m, 84.9°C	This study
ropB-up1	5′-ACA CAG ACA TCG ACT CGT GGA GGA TTC CCA TGC C-3′; upper primer for amplification of the 530-bp fragment with *ropB*; T_m, 89.3°C	This study
ropB-low	5′-TCG AAG CTT CAT CGC CTC GCC AC-3′; lower primer for amplification of the 530-bp fragment with *ropB*; T_m, 79.6°C	This study
Fkan	5′-CAC GTT GTG TCT CAA AAT CTC TGA TG-3′; upper primer for amplification of the 955-bp fragment containing Km^r cassette of pUC4K; T_m, 70.3°C	This study
Rkan	5′-TCT GCC AGT GTT ACA ACC AAT TAA CC-3′; lower primer for amplification of the 955-bp fragment containing Km^r cassette of pUC4K; T_m, 71.3°C	This study
rspLm1	5′-TTG TCG GGG CTT CTA CTT TCA TG-3′; *rspL* inactivation primer; T_m, 70.6°C	This study
rspLm2	5′-GAT TTT GAG ACA CAA CGT GTT TGA ACT TCT GCT GGT TGC G-3′; *rspL* inactivation primer; T_m, 89.8°C	This study
rspLm3	5′-GGT TGT AAC ACT GGC AGA GTG AAC AAC TCA AAC GAA GCG-3′; *rspL* inactivation primer; T_m, 88.8°C	This study
rspLm4	5′-GTT TGC TGG CCT CAT TGT GCT C-3′; *rspL* inactivation primer; T_m, 71.7°C	This study
rscVm1	5′-CTG TAT CTC CTG CCT GCT GAT CG-3′; *rscV* inactivation primer; T_m, 71.1°C	This study
rscVm2	5′-GAT TTT GAG ACA CAA CGT GAT CAT GCC GAC CGT AAA GC-3′; *rscV* inactivation primer; T_m, 89.2°C	This study
rscVm3	5′-GGT TGT AAC ACT GGC AGA GCA AGG AAA TCG CCC AGC-3′; *rscV* inactivation primer; T_m, 90.8°C	This study
rscVm4	5′-CAC ACA GAA GCG GAA CTC GTC G-3′; *rscV* inactivation primer; T_m, 72.6°C	This study
rscCm1	5′-GAC ACC CGA AGA GAA GCA GGA AG-3′; *rscC* inactivation primer; T_m, 71.6°C	This study
rscCm2	5′-GAT TTT GAG ACA CAA CGT GCG TCG ATT TCC ACC AGC TTG-3′; *rscC* inactivation primer; T_m, 91.6°C	This study
rscCm3	5′-GGT TGT AAC ACT GGC AGA GTT CAT TCA GGA CTA CGG CGA-3′; *rscC* inactivation primer; T_m, 89.7°C	This study
rscCm4	5′-GGT CAA GGG CGG AGA TGT AGC-3′; *rscC* inactivation primer; T_m, 70.6°C	This study
ropBm1	5′-CGC AAG GAG TTC AAG GAA ATG G-3′; *ropB* inactivation primer; T_m, 70.9°C	This study
ropBm2	5′-GAT TTT GAG ACA CAA CGT GCT CGT CAG GGG TCT GGG TTC-3′; *ropB* inactivation primer; T_m, 91.9°C	This study
ropBm3	5′-GGT TGT AAC ACT GGC AGA GGG GCA CCG ACA GCT TAT C-3′; *ropB* inactivation primer; T_m, 90.1°C	This study
ropBm4	5′-GGG TTA TGC AGG CTC ATC GCT TT-3′; *ropB* inactivation primer; T_m, 74.0°C	This study
rspHm1	5′-TAA AGG GTT GTC CAT GCT GGC-3′; *rspH* inactivation primer; T_m, 69.6°C	This study
rspHm2	5′-GAT TTT GAG ACA CAA CGT GAA GTA ATC GTG CAG GTA GGA C-3′; *rspH* inactivation primer; T_m, 86.3°C	This study
rspHm3	5′-GGT TGT AAC ACT GGC AGA CTA TTG GAA CCT GTC GTT GC-3′; *rspH* inactivation primer; T_m, 87.5°C	This study
rspHm4	5′-TCA CAC CCC TGG CGG CAC TAC-3′; *rspH* inactivation primer; T_m, 74.7°C	This study

[a] Rif^r, rifampin resistance; Gm^r, gentamicin resistance; Cm^r, chloramphenicol resistance; Zeo^r, zeocin resistance; Nal^r, nalidixic acid resistance; Km^r, kanamycin resistance; Sp^r, spectinomycin resistance; *aph*, aminoglycoside 3′-phosphotransferase; *aacC1*, gentamicin acetyltransferase 3-1; *bla*, β-lactamase; T_m, melting temperature calculated by Oligo 6.65 primer analysis software.

micin. To confirm transposon integration, the region flanking *att*Tn*7* was amplified by PCR with oligonucleotide primers P_{Tn7R} (17) and Q8glmS (Table 1), which are specific to the right end of the mini-Tn*7* element and the 3′ end of the glutamine synthetase gene of Q8r1-96, *glmS*, respectively.

Phenotypic characterization of *rsc*/*rsp* mutants. Mutants were assayed for growth kinetics in King's B and M9 media, swimming motility, and production of exoprotease, siderophore, and 2,4-DAPG as described earlier (41, 42). Long-term rhizosphere colonization assays were performed with wheat *Triticum aes-*

tivum L. cv. Penawawa and pea *Pisum sativum* L. cv. Columbia in raw soil as described by Landa et al. (35). Each mutant was tested in the colonization assay alone and in direct competition with the parental strain. For colonization assays, kanamycin- and gentamicin-resistant derivatives Q8r1-96Km and Q8r1-96Gm were used instead of the wild-type Q8r1-96 in order to distinguish strains in mixed inoculation treatments. Q8r1-96Km and Q8r1-96Gm were obtained by tagging the parental strain with disarmed transposons mini-Tn*7-gfp1* and mini-Tn*7-gfp2*, which integrate into a specific neutral intergenic attachment site and do not affect the competitiveness of Q8r1-96 in the plant rhizosphere (40, 41, 64).

Quincy virgin soil was inoculated with bacteria in a 1% suspension of methylcellulose to give ~1×10^4 CFU g^{-1} of soil. Mixed inoculation treatments contained a 1:1 mixture (~0.5×10^4 CFU g^{-1} of soil for each strain) of Q8r1-96Km or Q8r1-96Gm and mutant. Plants were incubated in a growth chamber for four successive 2-week cycles at 15 ± 1°C (wheat) or 22 ± 1°C (pea) with a 12-h photoperiod. After each cycle, six randomly selected plants were harvested and root samples were prepared to determine the population size of the inoculated bacteria. Each treatment was replicated three times, and the entire experiment was conducted twice. Population densities of introduced bacteria were enumerated by using a PCR-based dilution endpoint assay (22). In mixed inoculation treatments, variants tagged with mini-Tn7s (42) and the *rsc*/*rsp* mutant strains were distinguished by PCR with primers targeting Km^r and Gm^r genes. Bacterial growth was assessed after 72 h, with an optical density at 600 nm (OD_{600}) of ≥0.1 considered positive.

Take-all biocontrol assays were performed according to the method of Weller et al. (69). To prepare the oat kernel inoculum of *Gaeumannomyces graminis* var. *tritici*, 250 ml of oat grain and 300 ml of water were mixed in 1-liter flasks. The oat grain was autoclaved on two consecutive days, and each flask was inoculated with *G. graminis* var. *tritici* isolate ARS-A1 pregrown on 1/5× potato dextrose agar (PDA; BD, Sparks, MD) for 7 days. After 3 weeks of incubation at 23°C, the colonized oat grain was removed from the flasks, dried for 48 h under a sterile airflow, and then stored at 4°C. Colonized oat kernels were fragmented in a blender and sieved into particles of 0.25 to 1 mm. For biocontrol assays, 0.7% (wt/wt) of the *G. graminis* var. *tritici* ARS-A1 oat kernel inoculum was added to sieved and pasteurized Quincy virgin soil. Plastic tubes (15 cm long, 2.5-cm diameter) (Stuewe and Sons Inc., Corvallis, OR) were plugged with cotton balls and covered with a 6-cm column of autoclaved vermiculite and 10 g of inoculated soil. Each tube was watered with 12 ml of metalaxyl, after which three wheat seeds (*T. aestivum* L. cv. Penawawa) were sown into soil and covered with a 1-cm layer of vermiculite. The tubes (30 tubes per treatment in a completely randomized design) were placed in a growth room at 16°C with a 16-h photoperiod and covered with clear plastic bags until the plants emerged. Tubes received 6 ml of water twice a week and 1/3× Hoagland's nutrient solution (macroelements only) once a week. After 4 to 5 weeks, plants were removed from the tubes and the roots were washed and inspected for take-all lesions. Plants then were scored for height and take-all disease severity (0 to 8 scale, where "0" indicates no disease and "8" indicates a dead plant). The experiment was conducted twice.

Type III protein secretion assays. The pLN615 derivatives with cloned *ropAA*, *srcM*/*ropM*, and *srcB*/*ropB* genes were electroporated into DC3000 (pCPP2318), DC3000 *hrcC* (pCPP2318) or Q8rl-96 and used for type III protein secretion assays. The β-lactamases encoded by pCPP2318 and NPTII were used as lysis controls. Secretion assays were performed as previously described (51). Briefly, strains were grown for 6 h at 22°C in *hrp*-inducing conditions, after which the cultures were separated into cell and supernatant fractions by centrifugation. Secreted proteins in the supernatants were precipitated with trichloroacetic acid and washed with acetone. Proteins were separated by electrophoresis in a 12% sodium dodecyl sulfate-polyacrylamide gel and transferred onto polyvinylidene difluoride membranes for immunoblotting. The following primary antibodies were used: anti-hemagglutinin (HA) (Roche Diagnostics Corp., Indianapolis, IN), anti-β-lactamase (Chemicon International, Temecula, CA), and anti-NptII (Cortex Biochem, San Leandro, CA). Proteins on immunoblots were visualized using the CDP-Star chemiluminescence detection kit (Tropix, Bedford, MA) followed by autoradiography.

Adenylate cyclase injection assays. pENTR/D-TOPO plasmids *ropAA*, *srcB*/*ropB*, and *srcM*/*ropM* were used in Gateway LR reactions with Gateway destination vector pLN2193, which fuses genes with *cyaA*. These resultant constructs were electroporated into *P. fluorescens* 55(pLN1965). CyaA assays were performed as previously described (58). Briefly, bacteria were suspended in 5 mM morpholineethanesulfonic acid (MES) (pH 5.6) amended with 100 mM IPTG (isopropyl-β-D-thiogalactopyranoside) at an OD_{600} of 0.4 and infiltrated into leaves of *Nicotiana tabacum* cv. Xanthi. Disks of leaf tissue (0.7-cm diameter) were harvested 16 h after infiltration, and the concentration of cyclic AMP (cAMP) in each sample was measured using a direct cAMP enzyme immunoassay kit (Assay Designs, Ann Arbor, MI) by following the manufacturer's instructions.

Plant hypersensitive response assays. Constructs containing *ropAA*, *srcB*/*ropB*, or *srcM*/*ropM* were electroporated into *P. fluorescens* 55(pHIR11). Bacteria were suspended at 1×10^8 CFU ml^{-1} in 5 mM MES (pH 5.6) and used to prepare three 5-fold serial dilutions. The cell suspensions were infiltrated into *Nicotiana tabacum* cv. Xanthi leaves to determine the extent that they were able to suppress the HR caused by *P. fluorescens* 55(pHIR11). Strains containing pLN615 (an empty vector) or pLN347, a construct encoding AvrPtoB, were used as negative and positive controls, respectively. The HR was recorded and photographed 48 h after infiltration.

Measurement of reactive oxygen species (ROS). *P. fluorescens* 55(pLN1965) was electroporated with constructs that encoded RopAA, RopB, or RopM, each fused with a hemagglutinin (HA) tag at their C termini. These strains were separately infiltrated into *Nicotiana benthamiana* at a cell density of 2×10^8 CFU ml^{-1}. ROS measurements were done as described by Asai et al. (6). Briefly, disks of leaf tissue (0.4-cm diameter) were harvested from infiltrated leaf regions 15 h after infiltration and floated on water in wells of 96-well plates overnight. The water was replaced with a solution containing 0.5 mM chemiluminescence probe L-012 (Wako Pure Chemicals, Osaka, Japan), 10 mM morpholinepropanesulfonic acid (MOPS)/KOH (pH 7.4), and 1 mM flg22. Luminescence was measured using a GloMax Multi luminometer (Promega, Madison, WI).

Statistical analyses. All treatments in the growth chambers were arranged in a randomized complete block design. Data were analyzed by using STATISTIX v.8.0 (Analytical Software, Tallahassee, FL). Population data were converted to log CFU g^{-1} of root (fresh weight) or soil to satisfy the assumptions of analysis of variance (ANOVA). Differences in population densities among treatments were determined by standard ANOVA, and mean comparisons among treatments were performed by Fischer's protected least significance difference test ($P = 0.05$) or, when appropriate, by the Kruskal-Wallis test ($P = 0.05$).

Nucleotide sequence accession numbers. Sequence data were deposited in GenBank under accession numbers HM852191 through HM852211 for *rscRST* and HM854217 for 16S rRNA genes from STAD384.

RESULTS

Characterization of the *P. fluorescens* Q8r1-96 T3SS. While analyzing T3SS genes of Q8r1-96 we followed the naming convention introduced in *P. fluorescens* SBW25 by Preston et al. (53). Accordingly, type III structural and regulatory genes are named *rsp* (rhizosphere-expressed secretion protein) or *rsc* (rsp conserved), whereas type III effectors and their type III chaperones are named *rop* (rhizosphere-expressed outer protein) and *src* (specific Rop chaperone), respectively.

In *P. syringae*, expression of T3SS-related genes is mediated by the alternative sigma factor HrpL, which is thought to activate transcription in an RpoN-dependent manner by binding to a consensus bipartite promoter element, the "*hrp* box" (30). The *hrp* box motif is highly conserved and has been used as a reliable way to pinpoint the location of T3SS regulon genes in genomes of *P. syringae* and other bacterial species (24). Q8r1-96 carries *rspL*, a gene with similarity to *hrpL*, the product of which presumably forms the type III secretion regulatory circuit together with a putative RspL-specific response regulator, RspS, that is similar to the cognate response regulator HrpS of *P. syringae* pv. tomato DC3000 (Fig. 1; see Table S1 in the supplemental material). We manually examined regions upstream of Q8r1-96 *rspJ*, *rspF*, and *rspA* genes and identified additional putative *rsp* boxes (see Table S2 in the supplemental material). Since their structure closely resembled that of the consensus *hrp* box of *P. syringae* (KGGARCY[N_{15-16}]CCACNNA) (72), we built a hidden Markov model based on the aligned *hrp* boxes of strain DC3000 to screen the Q8r1-96 genome sequence.

The results of this screening yielded nine putative RspL-dependent promoters (see Table S2 in the supplemental ma-

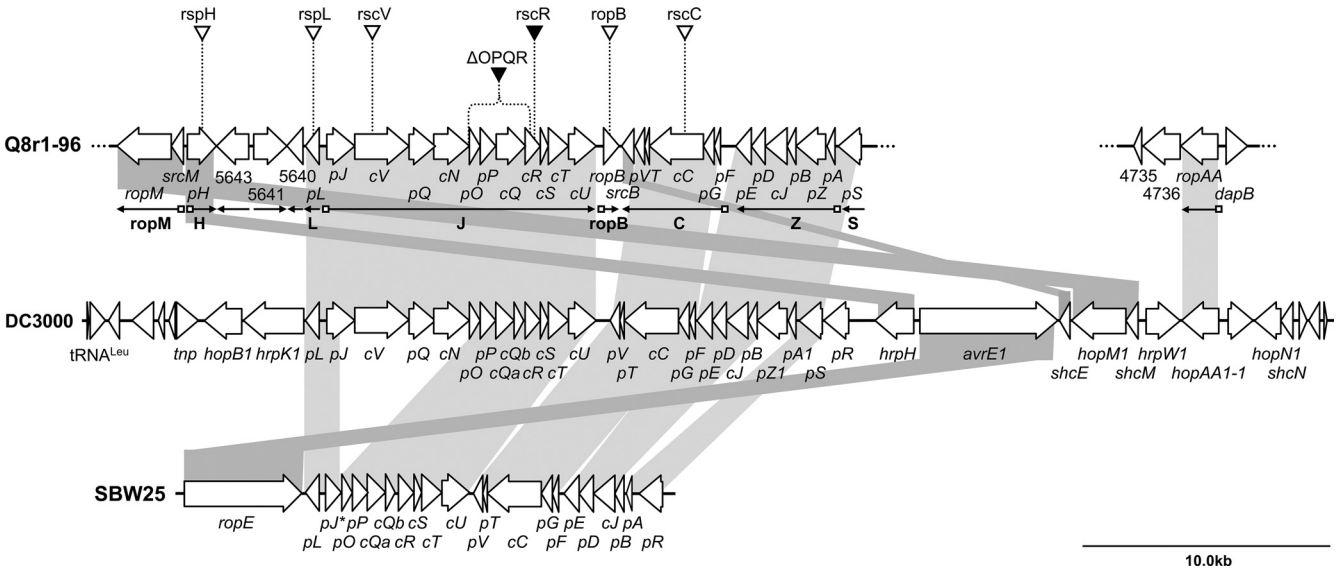

FIG. 1. Genetic organization of the type III secretion gene cluster and related genes in *P. fluorescens* Q8r1-96 (top) and its comparison to the *hrc*/*hrp* cluster of *P. syringae* pv. tomato DC3000 (1) (middle) and the *rsc*/*rsp* cluster of *P. fluorescens* SBW25 (53) (bottom). Predicted open reading frames and their orientation are shown by large arrows. Thin solid arrows and small rectangles indicate predicted transcripts and *rsp* boxes, respectively. Homologous genes are connected with gray shading. Insertions of Gm^r and Km^r cassettes in different mutants are indicated with inverted black and white triangles, respectively. Full gene names within *rsc*/*rsp* and *hrc*/*hrp* clusters were shortened and are indicated by a single letter preceded by "c" or "p" (corresponding to *rsc*/*hrc* or *rsp*/*hrp*, respectively). Some Q8r1-96 gene designations correspond to genome locus tags; e.g., the 5643 gene has locus tag PflQ8_5643.

terial). Six of these reside in the immediate vicinity of a 28.7-kb gene cluster similar to the *hrp*/*hrc* clusters of other plant-associated *Pseudomonas* spp. (Fig. 1). As mentioned above, three putative *rsp* boxes are found upstream of *rspA*, *rspF*, and *rspJ* genes and presumably drive expression of the Z, C, and J operons, which encode components of the T3SS machinery (Fig. 1; see Table S1 in the supplemental material). A fourth promoter is associated with the 1,272-bp *rscU-rspV* intergenic region, which contains convergently transcribed genes encoding the putative type III effector RopB and a putative type III chaperone SrcB (Fig. 1). Candidate *rsp* boxes are also found upstream of *rspH* and *srcM* that encode, respectively, a putative HrpH-like lytic murein transglycosylase and a putative type III chaperone for the product of *ropM*, a gene with similarity to the *P. syringae* effector gene *hopM1* (Fig. 1; Table S2). Finally, three additional *rsp* box motifs were identified upstream of genes PflQ8_4526 and PflQ8_5533, which encode a putative LysE-type efflux protein and a hemolysin III-like protein, respectively, and upstream of a putative type effector gene *ropAA*, which has strong similarity to *hopAA1-1* of *P. syringae* (Table S1). In addition to structural, effector, and regulatory genes, the Q8r1-96 T3S gene cluster also contains a gene encoding putative harpin-like translocator RspZ (Table S1). The overall arrangement of the *rsp*/*rsc* genes in Q8r1-96 differs from that in *P. fluorescens* SBW25 (53) and more closely resembles that of *P. syringae* (29) (Fig. 1).

Type III effectors of *P. fluorescens* Q8r1-96. Three putative type III effectors, RopAA, RopB, and RopM, were identified in the genome of *P. fluorescens* Q8r1-96 using blast similarity searches (see Table S1 in the supplemental material) and the following lines of evidence. All three putative Q8r1-96 type III effectors have composition typical of substrate proteins recognized by the T3SS (i.e., an amphipathic N-terminal part rich in Ser and polar residues, an aliphatic amino acid in position 3 or 4, and only one acidic residue in the first 12 positions) (see Table S3 in the supplemental material). Two of these genes, *ropM* and *ropB*, are found in the immediate vicinity of the *rsp*/*rsc* cluster and are accompanied by genes (*srcM* and *srcB*, respectively) encoding proteins with properties typically exhibited by type III chaperones. Finally, the putative promoters of all three type III effector genes contain well-conserved *rsp* box motifs (see Table S2 in the supplemental material).

The Q8r1-96 type III effector protein sequences were used to query the nonredundant data set of GenBank CDS translations, and the retrieved sequences were subjected to phylogenetic analyses. Database searches revealed that two of these effectors are members of the *P. syringae* HopAA1 and HopM1 type III effector families (38). Based on the similarity, these Q8r1-96 effectors were named RopAA and RopM, respectively. The NJ phylogeny estimated using available HopAA1 sequences revealed three major clades corresponding to proteins of *P. syringae*/*Pseudomonas viridiflava*, *Pseudomonas mendocina*, and *Ralstonia* spp. (Fig. 2A). The analysis also revealed that Q8r1-96 RopAA is only distantly related to its well-characterized *P. syringae* counterparts (25.5% identity; 38.6% similarity to HopAA1-1 of *P. syringae* pv. tomato DC3000) and more closely resembles putative type III effectors from *Ralstonia* spp. (30.4% identity; 40.9% similarity to RSIPO_04287 of *Ralstonia solanacearum* IPO1609). The RopM type III effector of Q8r1-96 also did not group with sequences from *P. syringae*/*P. viridiflava* (23.9% identity; 35.3% similarity to HopM1 of *P. syringae* pv. tomato DC3000) but rather formed a well-supported distinct clade (Fig. 2B). Finally, the third putative type III effector encoded by *ropB* bears no resemblance to

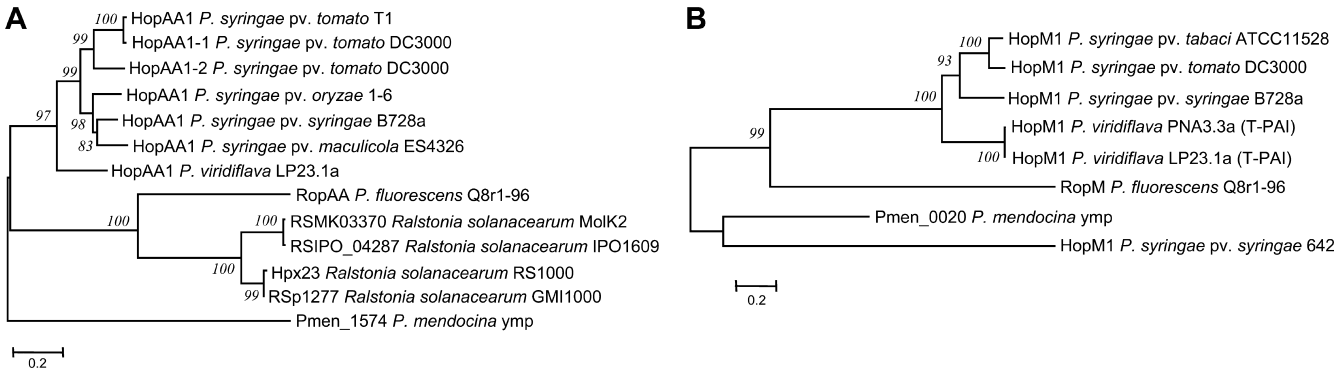

FIG. 2. Neighbor-joining phylogenies inferred from aligned protein sequences of the HopAA1 (A) and HopM1 (B) families. Indels were ignored in the analysis, and evolutionary distances were estimated using the Jones-Taylor-Thornton (JTT) model of amino acid substitution. Bootstrap values greater than 60% are shown, and the scale bar represents the number of substitutions per site. Branch lengths are proportional to the amount of evolutionary change.

known type III effectors. Iterative psi-blast searches revealed a very weak similarity to uncharacterized CRISPR-associated helicase Cas3 domain proteins from *Fusobacterium* spp. (data not shown).

Q8r1-96 represents a ubiquitous group of *P. fluorescens*-like strains with a distinct T3SS. We also investigated how the T3SS of Q8r1-96 is related to distinct variants of T3SSs previously described in plant-associated *Pseudomonas* spp. For this purpose, we estimated phylogenies of conserved HrcV, HrcR, HrcC, and HrcJ proteins, which each represent an individual operon of the T3SS gene cluster. The data set used for analyses ($n = 13$) included sequences from three *P. fluorescens*-like strains, eight strains of *P. syringae* and closely related species (i.e., *P. viridiflava* and *Pseudomonas cichorii*), and *P. mendocina*, a saprophytic soil- and rhizosphere-inhabiting organism closely related to *P. aeruginosa*. Neighbor-joining (NJ) phylogenies inferred from HrcV, HrcR, HrcC, and HrcJ protein sequences were highly congruent with each other and revealed that the *hrp*/*hrc* cluster of Q8r1-96 represents one of three distinct lineages (two other lineages are represented by entries from SBW25 and KD, respectively) of T3SSs found in *P. fluorescens*-like strains (see Fig. S1 in the supplemental material). Despite being diverse, individual Hrc sequences of Q8r1-96 always clustered together with those of SBW25, forming a well-supported clade. Comparison of Hrc-based phylogenies with that inferred from sequences of 16S rRNA genes revealed that strains Q8r1-96 and SBW25 are related but belong to two different groups of *P. fluorescens*-like species, thus agreeing with the results of Hrc-based analyses and suggesting that T3SSs of Q8r1-96 and SBW25 are likely evolved through vertical descent (Fig. S1). Our results also revealed that although *Pseudomonas* sp. strain KD is closely related to Q8r1-96, Hrc sequences of the former cluster consistently with their counterparts from *P. syringae*, *P. viridiflava*, and *P. mendocina* (Fig. S1). This finding strongly suggests the possibility of acquisition of the *hrp*/*hrc* gene cluster of *Pseudomonas* sp. KD via horizontal transfer and agrees with results previously reported by Rezzonico et al. (57).

The notion that the T3SSs of Q8r1-96 and SBW25 represent two distinct lineages is further supported by the fact that the *rsp*/*rsc* clusters of these strains are found in different chromosomal locations (see Fig. S2 in the supplemental material). In Q8r1-96, the cluster is flanked by genes PflQ8_5613 and PflQ8_5648, which encode conserved hypothetical and penicillin amidase-like proteins, respectively. Examination of other sequenced *P. fluorescens* genomes revealed that in strain Pf-01 (60) this spot is occupied by an S-pyocin gene cluster, whereas in strains Pf-5 (50) and SBW25 (60) the homologues of PflQ8_5613 and PflQ8_5648 flank each other directly (Fig. S2A). Interestingly, the integration site of the *rsp*/*rsc* genes in SBW25 is also conserved in *P. fluorescens* and is occupied in strains Pf-5 and Pf0-1 by a genomic island and a cluster of S-pyocin genes, respectively (Fig. S2B). In Q8r1-96, this site is flanked by genes PflQ8_0753 and *ychF* (PflQ8_5648) and is occupied by a 30.3-kb genomic island (unrelated to the one from Pf-5) that has low G+C content (54.1%) and includes, among other genes, those encoding a putative group II intron and a bacteriophage-like site-specific integrase (PflQ8_0767). The average G+C content of the Q8r1-96 T3SS cluster (63.0%) and putative effector genes *ropM* (59.8%), *ropB* (62.3%), and *ropAA* (62.9%) is similar to that of the genome (61.0%), and no abrupt shifts in G+C content are observed between *rsp*/*rsc* genes and flanking sequences (Fig. S2A). This differs from SBW25, where the average G+C content of the part of the T3SS cluster spanning *rspR* to *rspG* is significantly lower (52.0%) than the average content of the genome (59.9%) (53).

Finally, we used PCR with primers targeting *rscRST* genes to screen a set of biocontrol strains that share with Q8r1-96 the capacity to produce the antibiotic 2,4-DAPG but have been isolated worldwide from different crops. Results of the screening revealed that of 21 strains tested, only 1, CHA0, lacks T3SS genes (data not shown). The amplified *rscRST* DNA fragments were sequenced and used in phylogenetic analyses along with homologous sequences from other plant-associated pseudomonads ($n = 56$). Phylograms inferred by NJ analysis confirmed the presence of the three distinct lineages in species of the *P. fluorescens* group. The analysis also revealed that *rscRST* sequences of most 2,4-DAPG-producing *Pseudomonas* spp. are tightly clustered with their homologues from Q8r1-96 (see Fig. S3 in the supplemental material), thus suggesting that the

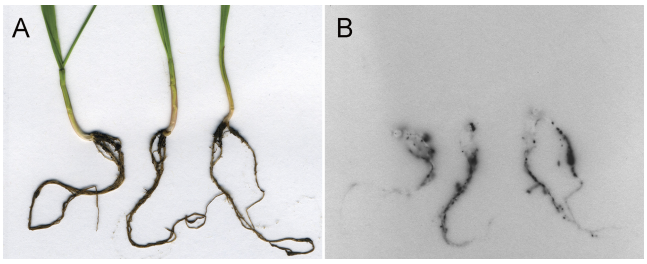

FIG. 3. Expression of Q8r1-96 T3SS genes in the rhizosphere of wheat grown in raw Quincy soil. Seeds were inoculated with ~10^6 CFU $seed^{-1}$ of *P. fluorescens* Q8r1-96rspJ-lux carrying mini-Tn*7* with the *rspJ* promoter fused to *luxCDABE* genes. (A) Wheat seedlings. (B) Roots exposed to X-ray film.

Q8r1-96-like lineage of T3SS genes is widely distributed among rhizosphere *Pseudomonas* spp.

The *rsc*/*rsp* genes of Q8r1-96 are expressed in the rhizosphere. To confirm that the T3SS locus is functional in the plant rhizosphere, we tagged Q8r1-96 with a mini-Tn*7* carrying the *rspJ* promoter fused to the operon encoding luciferase of *Photorhabdus luminescens* and used the resultant Q8r1-96rspJ-lux strain to treat seeds of wheat *T. aestivum* L. cv. Penawawa. The treated seeds were sown in pots containing raw Quincy virgin soil, and plants were grown in a growth chamber as described in Materials and Methods. After 10 days, plants were gently removed from pots, wrapped in clear plastic film, and exposed to X-ray film. Results of the assay confirmed that the T3SS genes of Q8r1-96 are indeed expressed in the rhizosphere of wheat (Fig. 3). No signal was detected in plants inoculated with the control strain carrying mini-Tn*7* with a promoterless luciferase operon (data not shown).

Effect of *rsc*/*rsp* mutations. To test the possible involvement of the T3SS in rhizosphere competence of Q8r1-96, we introduced mutations in *rspH*, *rspL*, *rscV*, *rscR*, *ropB*, and *hrcC* genes along with a deletion that spans *rspOP-rscQR* genes (Fig. 1). Homologs of each of these genes are required for a functional *P. syringae* T3SS (27, 28). The *rsc*/*rsp* mutant strains were tested *in vitro* for possible phenotypic changes in traits contributing to biocontrol by rhizosphere-dwelling *Pseudomonas* spp. All mutants were compared to the parental strain for the ability to grow in rich and minimal media, to produce exoprotease, siderophores, and the antibiotic 2,4-DAPG, and to spread on semisolid media. No phenotypic changes were associated with the introduced mutations, and the corresponding mutants did not differ significantly from Q8r1-96 in any of the aforementioned tests (data not shown). The mutant strains were also tested for the ability to persist in the plant rhizosphere by using competitive wheat root colonization assays in the greenhouse. Wheat and pea were sown into raw Quincy virgin soil inoculated with the mutant and parental strains introduced either individually or as a 1:1 mixture. The results indicated that inactivation of the *rsc*/*rsp* genes did not reduce the competitiveness of Q8r1-96, and populations of the mutants were similar to those of the parental strain (see Tables S4 and S5 in the supplemental material). We also tested whether the T3SS mutations impaired the ability of Q8r1-96 to suppress take-all disease of wheat. Wheat seeds were treated with Q8r1-96 or each of the five T3SS mutants and sown in pasteurized Quincy virgin soil inoculated with the take-all decline fungus. Disease severity ratings taken after 4 weeks of growth under controlled conditions indicated that plants colonized by the wild-type Q8r1-96 had significantly less ($P = 0.05$) disease (severity of ~4.0 on the 0-to-8 scale) than those from control treatments inoculated only with the take-all disease fungus *G. graminis* var. *tritici* (severity of 5.0). However, the inactivation of *rsc*/*rsp* genes did not result in a significant reduction in the biocontrol activity of Q8r1-96 (see Table S6 in the supplemental material).

Q8rl-96 type III effectors are secreted in culture from *P. syringae* and *P. fluorescens*. To determine whether the putative Q8r1-96 type III effectors RopAA, RopB, and RopM could be secreted in culture via a T3SS, we electroporated constructs carrying each of their genes fused at their 3′ termini to a hemagglutinin (HA) epitope into *P. syringae* pv. tomato DC3000 and *P. fluorescens* Q8r1-96. Importantly, the constructs encoding RopB-HA and RopM-HA also carried genes encoding their putative type III chaperones SrcB and SrcM, respectively. We included *P. syringae* secretion experiments because the protocols are well established whereas they are not for *P. fluorescens*. The strains were grown overnight in a rich liquid medium and then for 6 h in a minimal medium that induces the *P. syringae* type III secretion system (30). Cell-bound and supernatant fractions were subjected to sodium dodecyl sulfate-polyacrylamide gel electrophoresis (SDS-PAGE) and immunoblot analyses. RopAA-HA, RopB-HA, and RopM-HA were detected in supernatant fractions from wild-type DC3000 but not from a DC3000 *hrcC* mutant defective in type III secretion (Fig. 4A). These strains also expressed a mature form of β-lactamase, which was found only in the cell fractions, indicating that nonspecific cell lysis did not occur in significant amounts (Fig. 4A). RopAA-HA, RopB, and RopM were also found in the supernatant fractions in similar secretion experiments that used Q8r1-96 strains expressing these type III effectors (Fig. 4B). Taken together, the results indicate that these proteins are secreted in culture via the *P. syringae* and *P. fluorescens* T3Ss.

RopAA, RopB, and RopM are injected into plant cells by the *P. syringae* and *P. fluorescens* T3SSs. In the majority of cases, type III substrates that are secreted in culture by the T3SS of *P. syringae* are also injected into plant cells. To determine if Q8r1-96 type III effectors RopAA, RopB, and RopM are injected into leaf cells, we used an adenylate cyclase (CyaA) injection assay (58). This assay can determine if a type III effector-CyaA fusion is injected into eukaryotic cells because the CyaA enzyme is dependent on calmodulin, a protein present in sufficient amounts only inside eukaryotic cells. When a CyaA fusion is injected into plant cells there is a substantial increase in cAMP, a product of the CyaA-catalyzed reaction. We made constructs that express Q8r1-96 type III effectors C terminally fused to CyaA and electroporated these constructs into *P. fluorescens* 55(pLN1965) and *P. fluorescens* Q8r1-96. *P. fluorescens* 55(pLN1965) encodes a functional *P. syringae* T3SS, and it has been used to inject *P. syringae* type III effectors into plant leaf cells (25). We included *P. fluorescens* 55(pLN1965) in these experiments because we did not know if the native T3SS of Q8r1-96 would be capable of injecting type III effectors into leaf cells. Bacterial strains expressing RopAA-CyaA, RopB-CyaA, or RopM-CyaA were infiltrated

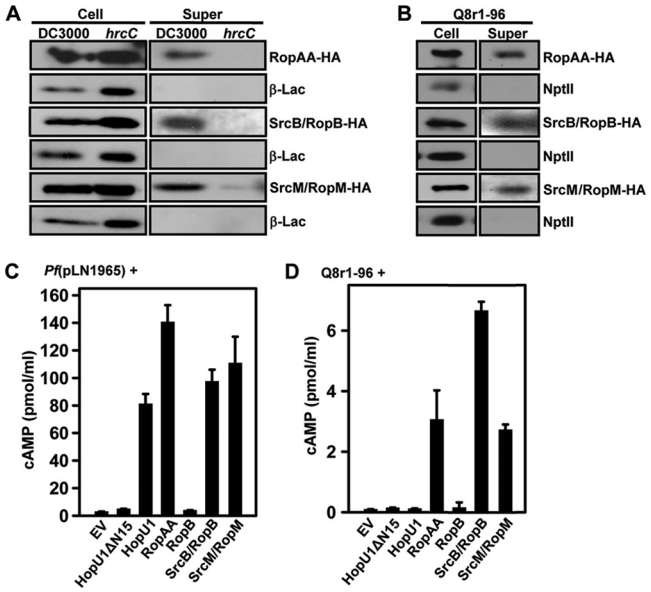

FIG. 4. Q8r1-96 type III effectors are secreted in culture (A and B) and injected into plant cells (C and D) by *P. syringae* and *P. fluorescens* T3SSs. (A) *P. syringae* pv. tomato DC3000 and a DC3000 *hrcC* mutant (defective in type III secretion) carrying constructs that expressed RopAA, RopB, or RopM fused at their C termini to a hemagglutinin (HA) epitope were grown under type III-inducing conditions. The cultures were separated into cell-bound (Cell) and supernatant (Super) fractions and subjected to SDS-PAGE and immunoblot analyses using anti-HA antibodies. These strains also contained the construct pCPP2318, which encodes a mature form of β-lactamase, a control for nonspecific leakage. The RopB-HA and RopM-HA constructs also encoded SrcB or SrcM, respectively, which are putative type III chaperones for these type III effectors. (B) *P. fluorescens* Q8r1-96 carrying the same constructs as those shown in panel A were grown under type III-inducing conditions, and the cultures were separated into cell-bound (Cell) and supernatant (Super) fractions and subjected to SDS-PAGE and immunoblot analyses using anti-HA antibodies. Neomycin phosphotransferase II (NptII), which is encoded by each construct, was used as a nonspecific leakage control. (C) *P. fluorescens* 55(pLN1965) strains carrying constructs that encode RopAA, RopB, or RopM fused at their C termini to adenylate cyclase (CyaA) were infiltrated into *N. tabacum* cv. Xanthi leaves, and after 16 h leaf disks were harvested and cyclic AMP (cAMP) levels were determined. The injection of RopB-CyaA was dependent on the presence of its type III chaperone SrcB. (D) *P. fluorescens* Q8r1-96 carrying the same constructs as those shown in panel C were infiltrated into *N. tabacum* cv. Xanthi leaves, and cAMP levels were determined. A strain carrying a construct encoding the *P. syringae* HopU1-CyaA was used as a positive control, and strains carrying an empty vector (EV) and a construct encoding a HopU1 derivative lacking its N-terminal 15 amino acids (HopU1ΔN15) were negative controls.

into *N. tabacum* cv. Xanthi (tobacco) leaves, and 16 h later cAMP levels were determined in harvested plant samples. Plant tissue infiltrated with *P. fluorescens* 55(pLN1965) expressing RopAA-CyaA, RopB-CyaA, or RopM-CyaA showed high levels of cAMP, indicating that each of these type III effectors was injected into tobacco leaf cells via the *P. syringae* T3SS (Fig. 4C). The strains that were capable of injecting RopB-CyaA and RopM-CyaA into plant cells also expressed their type III chaperones SrcB and SrcM, respectively. A strain that expressed RopB-CyaA without its type III chaperone SrcB was not injected in large amounts based on the low levels of cAMP (Fig. 4C), demonstrating that RopB is dependent on SrcB for it to be type III secreted.

Tobacco leaf tissue infiltrated with Q8r1-96 strains expressing the different CyaA fusions contained low levels of cAMP (Fig. 4D). However, the strains that expressed RopAA-CyaA, RopB-CyaA (with SrcB), and RopM-CyaA (with SrcM) contained significantly higher levels of cAMP than samples infiltrated with the control strains, indicating that the Q8r1-96 T3SS can inject these type III effectors into leaf cells (Fig. 4D), albeit at a much lower level than the *P. syringae* T3SS. It is important to note that *P. syringae* normally resides in the apoplast between leaf mesophyll cells whereas *P. fluorescens* is a soil bacterium normally present in the rhizoshere near plant roots. Thus, the Q8r1-96 T3SS may not sense the proper plant signals in leaves to fully engage its contact-dependent injection system.

RopAA, RopB, and RopM can suppress PAMP-triggered and effector-triggered immune responses. To determine if the Q8r1-96 type III effectors RopAA-CyaA, RopB-CyaA, and RopM-CyaA were capable of suppressing the innate immune response, we tested if they were able to suppress an HR, an ETI response, and flg22-induced reactive oxygen species (ROS) production, a PTI response. We used an established assay using strain *P. fluorescens* 55(pHIR11) to determine the extent that Q8r1-96 type III effectors could suppress the HopA1-dependent HR (25, 32). This strain can elicit an HR on tobacco and many other plants because it encodes a functional *P. syringae* T3SS and one type III effector, HopA1, which is recognized by tobacco and other plants inducing ETI (29). We introduced constructs that encoded these type III effectors (fused C terminally to an HA epitope) into *P. fluorescens* 55(pHIR11) and confirmed that they were expressed with immunoblot analyses (data not shown). Bacterial strains expressing these Q8r1-96 type III effectors did not elicit the HopA1-dependent HR when they were infiltrated at 2×10^7 cells/ml (Fig. 5A). However, they retained the ability to elicit the HopA1-dependent HR when the bacterial strains were infiltrated at 1×10^8 cells/ml (data not shown). This would designate them as class II suppressors using the grouping system described by Guo et al. (25).

To determine if the Q8r1-96 type III effectors could suppress a PTI response, we infiltrated *P. fluorescens* 55(pLN1965) expressing RopAA-HA, RopB-HA, or RopM-HA into *N. benthamiana* leaf tissue and then 24 h later ROS levels were determined after flg22 treatment. ROS levels were determined using the chemiluminescence probe L-012, a luminol derivative that measures superoxide anion. We found that plant tissue infiltrated with bacterial strains expressing Q8r1-96 type III effectors produced smaller amounts of ROS after flg22 treatment than did a bacterial control strain carrying an empty vector (Fig. 5B). Thus, RopAA-HA, RopB-HA, or RopM-HA can suppress flg22-induced ROS production, suggesting that these type III effectors can suppress PTI.

DISCUSSION

The results of our study revealed that Q8r1-96 carries a full-fledged T3SS consisting of structural proteins, dedicated regulatory proteins RspL and RspS, a putative harpin-like translocator, RspZ, an accessory lytic murein transglycosylase,

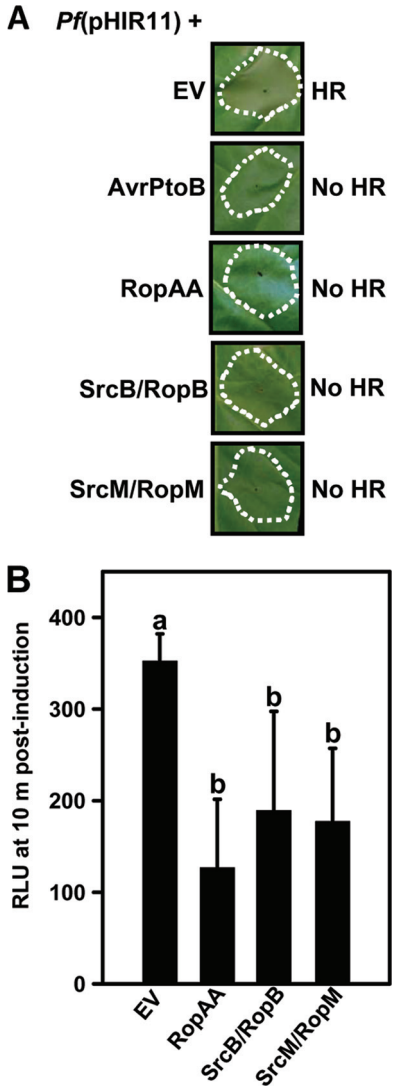

FIG. 5. Q8r1-96 type III effectors can suppress PTI and ETI responses. (A) *P. fluorescens* 55(pHIR11) strains carrying constructs that encode Q8r1-96 type III effectors RopAA-HA, RopB-HA, or RopM-HA were infiltrated into *N. tabacum* cv. Xanthi leaves at 1×10^7 cells/ml. Also infiltrated were *P. fluorescens* 55(pHIR11) strains with an empty vector (EV) or a construct that encoded the type III effector AvrPtoB, a *P. syringae* effector known to suppress the pHIR11-dependent HR. (B) ROS levels in *N. benthamiana* leaf tissue were determined 21 h after infiltration of *P. fluorescens* 55(pLN1965) strains carrying constructs that encode the Q8r1-96 type III effectors RopAA-HA, RopB-HA, or RopM-HA. The plant tissue was bathed in a flg22 solution while the ROS levels were being measured, and the relative light units (RLU) for the 10-min reading are shown. The standard errors are indicated with bars, and the results for the plant tissue infiltrated with the strain carrying the empty vector (EV) are significantly different from those for the strains expressing the Q8r1-96 type III effectors ($P < 0.02$).

RspH, and at least three type III effector proteins, RopM, RopAA, and RopB (see Table S1 in the supplemental material). The T3SS gene cluster appears to be stably fixed in the Q8r1-96 genome, a notion supported by the overall topological congruence among type III secretion and 16S rRNA genes and the lack of atypical G+C content, tRNAs, and site-specific integrase genes in the vicinity of the *rsc*/*rsp* genes (see Fig. S1 and S2 in the supplemental material). Our results also revealed that the T3SS of Q8r1-96 is different from its counterparts in the previously characterized biocontrol strains SBW25 (53) and KD (56) (Fig. S1) and that Q8r1-96-like T3SS genes are highly conserved among the majority of 2,4-DAPG-producing *Pseudomonas* spp. Taken together, these findings suggest that the *rsc*/*rsp* gene cluster of Q8r1-96 encodes a new distinct and conserved lineage of T3SSs, which is widely distributed among rhizosphere-dwelling *Pseudomonas* spp. that are associated with biological control of soilborne pathogens on a wide range of agricultural crops (66). The presence of stable divergent lineages of T3SSs in *P. fluorescens*-like strains is similar to the polymorphism of T3SSs observed in *P. viridiflava*, where the *hrc*/*hrp* genes are encoded by two distinct paralogous pathogenicity islands (PAIs), called T-PAI and S-PAI, that are integrated in different chromosome locations (4). The T-PAI- and S-PAI-carrying strains exhibit clear differences in virulence on *Arabidopsis thaliana* and tobacco, and it has been proposed that the stable maintenance of the two PAI types by selection may be beneficial for interaction of *P. viridiflava* with different hosts. Rhizosphere pseudomonads often strongly vary in their capacity to colonize roots of different plant species (66), and it is plausible that the presence of divergent lineages of T3SSs also reflects host specialization within *P. fluorescens*-like strains.

Over the past decade, considerable knowledge has been gained about the diversity and function of type III effectors in a wide range of animal- and plant-associated bacterial species (5). This makes comparative genome analyses useful and informative for providing clues about the identity of eukaryotic hosts targeted by a T3SS. The similarity of type III structural, regulatory, effector, and chaperone proteins of Q8r1-96 to their counterparts from *P. syringae* strongly suggests that the T3SS of Q8r1-96 is involved in interactions with the host plant. To test this hypothesis, we investigated whether the presence of functional *rsp*/*rsc* and effector genes is important for the ability of Q8r1-96 to multiply and persist in the plant rhizosphere and control the soilborne pathogen *G. graminis* var. *tritici*. Wheat and pea rhizosphere colonization assays performed in raw soil under greenhouse conditions revealed no difference between the population dynamics of several isogenic T3SS-deficient mutants and that of the parental strain (see Tables S4 and S5 in the supplemental material). Similarly, results of biocontrol assays revealed that the inactivation of T3SS genes did not impact the ability of Q8r1-96 to control take-all disease of wheat (see Table S6 in the supplemental material). The lack of a biocontrol phenotype associated with the T3SS mutants is surprising given the widespread occurrence and high level of conservation of the T3SS gene cluster in rhizosphere pseudomonads. We propose several explanations for these negative results. The type III effector-mediated suppression of PAMP recognition may be important for colonization of the plant rhizosphere only at early stages of the process, whereas our root colonization assays, which are tailored to estimate bacterial populations in the entire plant rhizosphere, may lack the sensitivity needed for detection of such transient changes in population levels. Root tip colonization assays may be more suitable for the detection of differences between the wild-type and mutant strains during initial steps in

rhizosphere colonization. We are currently establishing this assay to evaluate the Q8r1-96 T3SS mutants. It is also possible that type III effectors play a role in the interaction of Q8r1-96 with a plant host other than wheat and pea, which were evaluated in this study. The lack of an impact on the biocontrol capacity of Q8r1-96 may be due to the fact that production of the antibiotic 2,4-DAPG, which is the primary mechanism of inhibition of the take-all fungus in *P. fluorescens*, was unaffected in the *rsp*/*rsc* mutants. These data partially agree with results reported by other groups studying the T3SSs of saprophytic plant-associated *Pseudomonas* spp. For example, the interruption of *hrcV* in *P. fluorescens* KD diminished biological control of the soilborne pathogen *Pythium ultimum* but did not affect the persistence of the bacterium in the rhizosphere of cucumber (56). Finally, the presence of a hemolysin-like gene preceded by a well-conserved *rsp* box motif (see Tables S1 and S2 in the supplemental material) suggests another, yet unproven, role for the T3SS in Q8r1-96. Assuming that the aforementioned protein is indeed coexpressed with the T3SS and functions as a hemolysin, it is plausible that the resulting cytotoxic activity may enhance the ability of Q8r1-96 to resist bacteriovore predation in soil and this would not have been detected in our assays. Interestingly, a recent study by Sperandio et al. (61) demonstrated the involvement of a *P. syringae*-like T3SS gene cluster in hemolysin secretion by an unusual clinical strain of *P. fluorescens*.

In spite of the fact that we were unable to identify a role for the Q8r1-96 T3SS in the rhizosphere colonization and biocontrol properties of Q8r1-96, the results of our reporter assays reveal that type III secretion genes are expressed in the rhizosphere of wheat—the natural habitat of this organism (Fig. 3). The results of our functional assays also prove that the T3SS of Q8r1-96 is fully functional and capable of secreting and translocating cognate type III effectors (Fig. 4). Most interestingly, the results of our functional assays also prove unequivocally that RopB, RopM, and RopAA operate in Q8r1-96 as type III effectors, are secreted via the T3SS, and, upon entry into the host plant cells, are capable of suppressing both PTI and ETI (Fig. 5).

These type III effectors are of particular interest since they may provide clues about the molecular signaling that takes place during root colonization by T3SS$^+$ plant growth-promoting bacteria. RopM and RopAA belong to ancient type III effector families (38), and their *P. syringae* homologs (HopM1 and HopAA1-1) have been shown to suppress both ETI and PTI immune responses (9, 20, 25, 37, 48). While the enzymatic activities of HopM1 and HopAA1-1 are not known, HopM1 has been shown to induce the degradation of several host proteins via the plant 26S proteasome (47). One of these protein targets is AtMIN7, a key component of the vesicle trafficking system in plants, which would likely be involved in the delivery of immunity-related products outside plant cells during the plant's immune response. The similarity of RopM and RopAA to HopM1 and HopAA1-1, respectively, suggests that the Q8r1-96 type III effectors act inside plant cells and that they may possess activities similar to those of their *P. syringae* counterparts. Our results demonstrating that these proteins can also suppress plant immunity further support this possibility. Because the Q8r1-96 type III effector RopB is unlike any known type III effector and has no predicted homologs in the available sequenced bacterial genomes, less is known about its role in plants. However, since it has the ability to be secreted via the T3SS and it can suppress innate immune responses similarly to RopM and RopAA, it is likely to also act inside plant cells. Since RopB is not found in the type III effector inventory of plant pathogens, it is tempting to speculate that RopB may have targets that are root cell specific.

Since PAMPs of beneficial rhizobacteria act as common elicitors of induced systemic resistance (ISR) in plants (21), our data regarding the suppression of PTI and ETI immune responses by type III effectors are seemingly in conflict with the capacity of Q8r1-96 to induce the systemic resistance in *Arabidopsis thaliana* to *P. syringae* pv. tomato DC3000 (68). One plausible explanation for this contradiction is that the ISR effect of Q8r1-96 is mediated primarily by the polyketide metabolite 2,4-DAPG. 2,4-DAPG produced by *Pseudomonas* spp. is primarily known as an antibiotic involved in the suppressiveness of some soils to plant pathogens (66). However, recent studies have also demonstrated that DAPG produced by *P. fluorescens* can induce resistance in plants against *P. syringae* (66), oomycetes (31), and plant-parasitic nematodes (59), presumably by interfering with auxin signaling (13).

To summarize, our findings suggest for the first time the T3SS-mediated suppression of innate immunity by a rhizosphere-inhabiting strain of *P. fluorescens*. We also demonstrated that genes within the T3SS cluster are conserved among a large and diverse group of rhizosphere pseudomonads. The results of this study add to our understanding of the complex effects exerted by saprophytic bacteria on their plant hosts and raise questions about the diversity in type III effector repertoires in rhizosphere T3SS$^+$ bacteria and immune responses targeted by these effectors in root tissue.

ACKNOWLEDGMENTS

We thank Karen Hansen for technical assistance and Ming-Ming Yang for the help with take-all disease assays. We also gratefully acknowledge Ed Davis (Oregon State University), who contributed to the bioinformatic analyses of the type III secretion locus and effector loci of Q8r1-96.

The research in the Alfano laboratory was supported by grants from the U.S. Department of Agriculture (award no. 2007-35319-18336) and the National Institutes of Health (award no. 1R01AI069146-01A2) and funds from the Center for Plant Science Innovation at the University of Nebraska. The genomic sequencing of Q8r1-96 was supported by a grant to J.E.L. and I.T.P. from the U.S. Department of Agriculture, National Institute of Food and Agriculture (award no. 2008-35600-18770).

REFERENCES

1. **Alfano, J. R., A. O. Charkowski, W. L. Deng, J. L. Badel, T. Petnicki-Ocwieja, K. van Dijk, and A. Collmer.** 2000. The *Pseudomonas syringae* Hrp pathogenicity island has a tripartite mosaic structure composed of a cluster of type III secretion genes bounded by exchangeable effector and conserved effector loci that contribute to parasitic fitness and pathogenicity in plants. Proc. Natl. Acad. Sci. U. S. A. **97:**4856–4861.
2. **Alfano, J. R., and A. Collmer.** 1997. The type III (Hrp) secretion pathway of plant pathogenic bacteria: trafficking harpins, Avr proteins, and death. J. Bacteriol. **179:**5655–5662.
3. **Alfano, J. R., and A. Collmer.** 2004. Type III secretion system effector proteins: double agents in bacterial disease and plant defense. Annu. Rev. Phytopathol. **42:**385–414.
4. **Araki, H., D. Tian, E. M. Goss, K. Jakob, S. S. Halldorsdottir, M. Kreitman, and J. Bergelson.** 2006. Presence/absence polymorphism for alternative pathogenicity islands in *Pseudomonas viridiflava*, a pathogen of *Arabidopsis*. Proc. Natl. Acad. Sci. U. S. A. **103:**5887–5892.
5. **Arnold, R., A. Jehl, and T. Rattei.** 2010. Targeting effectors: the molecular recognition of type III secreted proteins. Microbes Infect. **12:**346–358.

6. **Asai, S., K. Ohta, and H. Yoshioka.** 2008. MAPK signaling regulates nitric oxide and NADPH oxidase-dependent oxidative bursts in *Nicotiana benthamiana*. Plant Cell **20:**1390–1406.
7. **Ausubel, F. M.** 2005. Are innate immune signaling pathways in plants and animals conserved? Nat. Immunol. **6:**973–979.
8. **Ausubel, F. M., R. Brent, R. E. Kingston, D. D. Moore, J. G. Seidman, J. A. Smith, and K. Struhl.** 2002. Short protocols in molecular biology, 5th ed. John Wiley and Sons, New York, NY.
9. **Badel, J. L., R. Shimizu, H. S. Oh, and A. Collmer.** 2006. A *Pseudomonas syringae* pv. tomato *avrE1/hopM1* mutant is severely reduced in growth and lesion formation in tomato. Mol. Plant Microbe Interact. **19:**99–111.
10. **Bennett-Lovsey, R. M., A. D. Herbert, M. J. Sternberg, and L. A. Kelley.** 2008. Exploring the extremes of sequence/structure space with ensemble fold recognition in the program Phyre. Proteins **70:**611–625.
11. **Block, A., G. Li, Z. Q. Fu, and J. R. Alfano.** 2008. Phytopathogen type III effector weaponry and their plant targets. Curr. Opin. Plant Biol. **11:**396–403.
12. **Boller, T., and G. Felix.** 2009. A renaissance of elicitors: perception of microbe-associated molecular patterns and danger signals by pattern-recognition receptors. Annu. Rev. Plant Biol. **60:**379–406.
13. **Brazelton, J. N., E. E. Pfeufer, T. A. Sweat, B. B. Gardener, and C. Coenen.** 2008. 2,4-Diacetylphloroglucinol alters plant root development. Mol. Plant Microbe Interact. **21:**1349–1358.
14. **Buttner, D., and S. Y. He.** 2009. Type III protein secretion in plant pathogenic bacteria. Plant Physiol. **150:**1656–1664.
15. **Charkowski, A. O., H.-C. Huang, and A. Collmer.** 1997. Altered localization of HrpZ in *Pseudomonas syringae* pv. syringae *hrp* mutants suggests that different components of the type III secretion pathway control protein translocation across the inner and outer membranes of gram-negative bacteria. J. Bacteriol. **179:**3866–3874.
16. **Choi, K. H., and H. P. Schweizer.** 2005. An improved method for rapid generation of unmarked *Pseudomonas aeruginosa* deletion mutants. BMC Microbiol. **5:**30.
17. **Choi, K. H., and H. P. Schweizer.** 2006. Mini-Tn*7* insertion in bacteria with single *att*Tn*7* sites: example *Pseudomonas aeruginosa*. Nat. Protoc. **1:**153–161.
18. **Cornelis, G. R.** 2010. The type III secretion injectisome, a complex nanomachine for intracellular "toxin" delivery. Biol. Chem. **391:**745–751.
19. **Cuppels, D. A.** 1986. Generation and characterization of Tn*5* insertion mutations in *Pseudomonas syringae* pv. *tomato.* Appl. Environ. Microbiol. **51:**323–327.
20. **DebRoy, S., R. Thilmony, Y. B. Kwack, K. Nomura, and S. Y. He.** 2004. A family of conserved bacterial effectors inhibits salicylic acid-mediated basal immunity and promotes disease necrosis in plants. Proc. Natl. Acad. Sci. U. S. A. **101:**9927–9932.
21. **De Vleesschauwer, D., and M. Hofte.** 2009. Rhizobacteria-induced systemic resistance. Adv. Bot. Res. **51:**223–281.
22. **Gardener, B. B. M., D. V. Mavrodi, L. S. Thomashow, and D. M. Weller.** 2001. A rapid polymerase chain reaction-based assay characterizing rhizosphere populations of 2,4-diacetylphloroglucinol-producing bacteria. Phytopathology **91:**44–54.
23. **Gardy, J. L., M. R. Laird, F. Chen, S. Rey, C. J. Walsh, M. Ester, and F. S. L. Brinkman.** 2005. PSORTb v. 2.0: expanded prediction of bacterial protein subcellular localization and insights gained from comparative proteome analysis. Bioinformatics **21:**617–623.
24. **Greenberg, J. T., and B. A. Vinatzer.** 2003. Identifying type III effectors of plant pathogens and analyzing their interaction with plant cells. Curr. Opin. Microbiol. **6:**20–28.
25. **Guo, M., F. Tian, Y. Wamboldt, and J. R. Alfano.** 2009. The majority of the type III effector inventory of *Pseudomonas syringae* pv. tomato DC3000 can suppress plant immunity. Mol. Plant Microbe Interact. **22:**1069–1080.
26. **Hoang, T. T., R. R. Karkhoff-Schweizer, A. J. Kutchma, and H. P. Schweizer.** 1998. A broad-host-range Flp-FRT recombination system for site-specific excision of chromosomally-located DNA sequences: application for isolation of unmarked *Pseudomonas aeruginosa* mutants. Gene **212:**77–86.
27. **Huang, H. C., S. Y. He, D. W. Bauer, and A. Collmer.** 1992. The *Pseudomonas syringae* pv. syringae 61 *hrpH* product, an envelope protein required for elicitation of the hypersensitive response in plants. J. Bacteriol. **174:**6878–6885.
28. **Huang, H. C., S. W. Hutcheson, and A. Collmer.** 1991. Characterization of the *hrp* cluster from *Pseudomonas syringae pv. syringae* 61 and Tn*phoA* tagging of genes encoding exported or membrane-spanning Hrp proteins. Mol. Plant Microbe Interact. **4:**469–476.
29. **Huang, H. C., R. Schuurink, T. P. Denny, M. M. Atkinson, C. J. Baker, I. Yucel, S. W. Hutcheson, and A. Collmer.** 1988. Molecular cloning of a *Pseudomonas syringae* pv. *syringae* gene cluster that enables *Pseudomonas fluorescens* to elicit the hypersensitive response in tobacco plants. J. Bacteriol. **170:**4748–4756.
30. **Huynh, T. V., D. Dahlbeck, and B. J. Staskawicz.** 1989. Bacterial blight of soybean: regulation of a pathogen gene determining host cultivar specificity. Science **245:**1374–1377.
31. **Iavicoli, A., E. Boutet, A. Buchala, and J. P. Metraux.** 2003. Induced systemic resistance in *Arabidopsis thaliana* in response to root inoculation with *Pseudomonas fluorescens* CHA0. Mol. Plant Microbe Interact. **16:**851–858.
32. **Jamir, Y., M. Guo, H. S. Oh, T. Petnicki-Ocwieja, S. Chen, X. Tang, M. B. Dickman, A. Collmer, and J. R. Alfano.** 2004. Identification of *Pseudomonas syringae* type III effectors that can suppress programmed cell death in plants and yeast. Plant J. **37:**554–565.
33. **Jones, J. D., and J. L. Dangl.** 2006. The plant immune system. Nature **444:**323–329.
34. **King, E. O., M. K. Ward, and D. E. Raney.** 1954. Two simple media for the demonstration of pyocyanin and fluorescein. J. Lab. Clin. Med. **44:**301–307.
35. **Landa, B. B., D. M. Mavrodi, L. S. Thomashow, and D. M. Weller.** 2003. Interactions between strains of 2,4-diacetylphloroglucinol-producing *Pseudomonas fluorescens* in the rhizosphere of wheat. Phytopathology **93:**982–994.
36. **Larkin, M. A., G. Blackshields, N. P. Brown, R. Chenna, P. A. McGettigan, H. McWilliam, F. Valentin, I. M. Wallace, A. Wilm, R. Lopez, J. D. Thompson, T. J. Gibson, and D. G. Higgins.** 2007. Clustal W and Clustal X version 2.0. Bioinformatics **23:**2947–2948.
37. **Li, X., H. Lin, W. Zhang, Y. Zou, J. Zhang, X. Tang, and J. M. Zhou.** 2005. Flagellin induces innate immunity in nonhost interactions that is suppressed by *Pseudomonas syringae* effectors. Proc. Natl. Acad. Sci. U. S. A. **102:**12990–12995.
38. **Lindeberg, M., J. Stavrinides, J. H. Chang, J. R. Alfano, A. Collmer, J. L. Dangl, J. T. Greenberg, J. W. Mansfield, and D. S. Guttman.** 2005. Proposed guidelines for a unified nomenclature and phylogenetic analysis of type III Hop effector proteins in the plant pathogen *Pseudomonas syringae*. Mol. Plant Microbe Interact. **18:**275–282.
39. **Marchler-Bauer, A., and S. H. Bryant.** 2004. CD-Search: protein domain annotations on the fly. Nucleic Acids Res. **32:**W327–W331.
40. **Mavrodi, O. V., B. B. M. Gardener, D. V. Mavrodi, R. F. Bonsall, D. M. Weller, and L. S. Thomashow.** 2001. Genetic diversity of *phlD* from 2,4-diacetylphloroglucinol-producing fluorescent *Pseudomonas* spp. Phytopathology **91:**35–43.
41. **Mavrodi, O. V., D. V. Mavrodi, A. A. Park, D. M. Weller, and L. S. Thomashow.** 2006. The role of *dsbA* in colonization of the wheat rhizosphere by *Pseudomonas fluorescens* Q8r1-96. Microbiology **152:**863–872.
42. **Mavrodi, O. V., D. V. Mavrodi, D. M. Weller, and L. S. Thomashow.** 2006. Role of *ptsP*, *orfT*, and *sss* recombinase genes in root colonization by *Pseudomonas fluorescens* Q8r1-96. Appl. Environ. Microbiol. **72:**7111–7122.
43. **Mazurier, S., M. Lemunier, S. Siblot, C. Mougel, and P. Lemanceau.** 2004. Distribution and diversity of type III secretion system-like genes in saprophytic and phytopathogenic fluorescent pseudomonads. FEMS Microbiol. Ecol. **49:**455–467.
44. **Medzhitov, R., and C. A. Janeway.** 1997. Innate immunity: the virtues of a nonclonal system of recognition. Cell **91:**295–298.
45. **Millet, Y. A., C. H. Danna, N. K. Clay, W. Songnuan, M. D. Simon, D. Werck-Reichhart, and F. M. Ausubel.** 2010. Innate immune responses activated in Arabidopsis roots by microbe-associated molecular patterns. Plant Cell **22:**973–990.
46. **Nicaise, V., M. Roux, and C. Zipfel.** 2009. Recent advances in PAMP-triggered immunity against bacteria: pattern recognition receptors watch over and raise the alarm. Plant Physiol. **150:**1638–1647.
47. **Nomura, K., S. Debroy, Y. H. Lee, N. Pumplin, J. Jones, and S. Y. He.** 2006. A bacterial virulence protein suppresses host innate immunity to cause plant disease. Science **313:**220–223.
48. **Oh, H. S., and A. Collmer.** 2005. Basal resistance against bacteria in *Nicotiana benthamiana* leaves is accompanied by reduced vascular staining and suppressed by multiple *Pseudomonas syringae* type III secretion system effector proteins. Plant J. **44:**348–359.
49. **Pagni, M., V. Ionnidis, L. Cerutti, M. Zahn-Zabal, C. V. Jongeneel, and L. Falquet.** 2004. Myhits: a new interactive resource for protein annotation and domain identification. Nucleic Acids Res. **32:**W332–W335.
50. **Paulsen, I. T., C. M. Press, J. Ravel, D. Y. Kobayashi, G. S. A. Myers, D. V. Mavrodi, R. T. DeBoy, R. Seshadri, Q. H. Ren, R. Madupu, R. J. Dodson, A. S. Durkin, L. M. Brinkac, S. C. Daugherty, S. A. Sullivan, M. J. Rosovitz, M. L. Gwinn, L. W. Zhou, D. J. Schneider, S. W. Cartinhour, W. C. Nelson, J. Weidman, K. Watkins, K. Tran, H. Khouri, E. A. Pierson, L. S. Pierson, L. S. Thomashow, and J. E. Loper.** 2005. Complete genome sequence of the plant commensal *Pseudomonas fluorescens* Pf-5. Nat. Biotechnol. **23:**873–878.
51. **Petnicki-Ocwieja, T., D. J. Schneider, V. C. Tam, S. T. Chancey, L. Shan, Y. Jamir, L. M. Schechter, M. D. Janes, C. R. Buell, X. Tang, A. Collmer, and J. R. Alfano.** 2002. Genomewide identification of proteins secreted by the Hrp type III protein secretion system of *Pseudomonas syringae* pv. tomato DC3000. Proc. Natl. Acad. Sci. U. S. A. **99:**7652–7657.
52. **Preston, G. M.** 2007. Metropolitan microbes: type III secretion in multihost symbionts. Cell Host Microbe **2:**291–294.
53. **Preston, G. M., N. Bertrand, and P. B. Rainey.** 2001. Type III secretion in plant growth-promoting *Pseudomonas fluorescens* SBW25. Mol. Microbiol. **41:**999–1014.
54. **Raaijmakers, J. M., and D. M. Weller.** 1998. Natural plant protection by 2,4-diacetylphloroglucinol-producing *Pseudomonas* spp. in take-all decline soils. Mol. Plant Microbe Interact. **11:**144–152.

55. **Rainey, P. B.** 1999. Adaptation of *Pseudomonas fluorescens* to the plant rhizosphere. Environ. Microbiol. **1:**243–257.
56. **Rezzonico, F., C. Binder, G. Defago, and Y. Moenne-Loccoz.** 2005. The type III secretion system of biocontrol *Pseudomonas fluorescens* KD targets the phytopathogenic Chromista *Pythium ultimum* and promotes cucumber protection. Mol. Plant Microbe Interact. **18:**991–1001.
57. **Rezzonico, F., G. Defago, and Y. Moenne-Loccoz.** 2004. Comparison of ATPase-encoding type III secretion system *hrcN* genes in biocontrol fluorescent pseudomonads and in phytopathogenic proteobacteria. Appl. Environ. Microbiol. **70:**5119–5131.
58. **Schechter, L. M., K. A. Roberts, Y. Jamir, J. R. Alfano, and A. Collmer.** 2004. *Pseudomonas syringae* type III secretion system targeting signals and novel effectors studied with a Cya translocation reporter. J. Bacteriol. **186:**543–555.
59. **Siddiqui, I. A., and S. S. Shaukat.** 2004. Systemic resistance in tomato induced by biocontrol bacteria against the root-knot nematode, Meloidogyne javanica is independent of salicylic acid production. J. Phytopathol. **152:**48–54.
60. **Silby, M. W., A. M. Cerdeno-Tarraga, G. S. Vernikos, S. R. Giddens, R. W. Jackson, G. M. Preston, X. X. Zhang, C. D. Moon, S. M. Gehrig, S. A. Godfrey, C. G. Knight, J. G. Malone, Z. Robinson, A. J. Spiers, S. Harris, G. L. Challis, A. M. Yaxley, D. Harris, K. Seeger, L. Murphy, S. Rutter, R. Squares, M. A. Quail, E. Saunders, K. Mavromatis, T. S. Brettin, S. D. Bentley, J. Hothersall, E. Stephens, C. M. Thomas, J. Parkhill, S. B. Levy, P. B. Rainey, and N. R. Thomson.** 2009. Genomic and genetic analyses of diversity and plant interactions of *Pseudomonas fluorescens*. Genome Biol. **10:**R51.
61. **Sperandio, D., G. Rossignol, J. Guerillon, N. Connil, N. Orange, M. G. Feuilloley, and A. Merieau.** 2010. Cell-associated hemolysis activity in the clinical strain of *Pseudomonas fluorescens* MFN1032. BMC Microbiol. **10:** 124.
62. **Tampakaki, A. P., N. Skandalis, A. D. Gazi, M. N. Bastaki, P. F. Sarris, S. N. Charova, M. Kokkinidis, and N. J. Panopoulos.** 2010. Playing the "harp": evolution of our understanding of *hrp*/*hrc* genes. Annu. Rev. Phytopathol. **48:**347–370.
63. **Tamura, K., J. Dudley, M. Nei, and S. Kumar.** 2007. MEGA4: Molecular Evolutionary Genetics Analysis (MEGA) software version 4.0. Mol. Biol. Evol. **24:**1596–1599.
64. **Troisfontaines, P., and G. R. Cornelis.** 2005. Type III secretion: more systems than you think. Physiology **20:**326–339.
65. **Validov, S., O. Mavrodi, L. De La Fuente, A. Boronin, D. Weller, L. Thomashow, and D. Mavrodi.** 2005. Antagonistic activity among 2,4-diacetylphloroglucinol-producing fluorescent *Pseudomonas* spp. FEMS Microbiol. Lett. **242:**249–256.
66. **Weller, D. M., B. B. Landa, O. V. Mavrodi, K. L. Schroeder, L. De La Fuente, S. Blouin Bankhead, R. Allende-Molar, R. F. Bonsall, D. V. Mavrodi, and L. S. Thomashow.** 2007. Role of 2,4-diacetylphloroglucinol-producing fluorescent *Pseudomonas* spp. in plant defense. Plant Biol. **9:**4–20.
67. **Weller, D. M., J. M. Raaijmakers, B. B. M. Gardener, and L. S. Thomashow.** 2002. Microbial populations responsible for specific soil suppressiveness to plant pathogens. Annu. Rev. Phytopathol. **40:**309–348.
68. **Weller, D. M., J. A. van Pelt, D. V. Mavrodi, C. M. J. Pieterse, P. A. H. M. Bakker, and L. C. van Loon.** 2004. Induced systemic resistance (ISR) in *Arabidopsis* against *Pseudomonas syringae* pv. tomato by 2,4-diacetylphloroglucinol (DAPG)-producing *Pseudomonas fluorescens.* Phytopathology **94:** S108.
69. **Weller, D. M., B.-X. Zhang, and R. J. Cook.** 1985. Application of a rapid screening test for selection of bacteria suppressive to take-all of wheat. Plant Dis. **69:**710–713.
70. **Yuan, J., and S. Y. He.** 1996. The *Pseudomonas syringae* Hrp regulation and secretion system controls the production and secretion of multiple extracellular proteins. J. Bacteriol. **178:**6399–6402.
71. **Zhou, J. M., and J. Chai.** 2008. Plant pathogenic bacterial type III effectors subdue host responses. Curr. Opin. Microbiol. **11:**179–185.
72. **Zwiesler-Vollick, J., A. E. Plovanich-Jones, K. Nomura, S. Bandyopadhyay, V. Joardar, B. N. Kunkel, and S. Y. He.** 2002. Identification of novel *hrp*-regulated genes through functional genomic analysis of the *Pseudomonas syringae* pv. tomato DC3000 genome. Mol. Microbiol. **45:**1207–1218.